Published in final edited form as:
Nanomedicine. 2014 July ; 10(5): 991–1002. doi:10.1016/j.nano.2014.02.004.

Lipid-Polymer Nanoparticles Encapsulating Curcumin for Modulating the Vascular Deposition of Breast Cancer Cells

Anna L. Palange, M.Sc.[1,2], **Daniele Di Mascolo, M.Sc.**[1,2], **Claudio Carallo, M.D.**[2], **Agostino Gnasso, M.D.**[2], and **Paolo Decuzzi, Ph.D.**[1,2,*]

[1]Department of Translational Imaging and Department of Nanomedicine, Houston Methodist Research Institute, Houston , TX 77030, USA

[2]Department of Experimental and Clinical Medicine, University of Magna Graecia, Catanzaro 88100, Italy

Abstract

Vascular adhesion and endothelial transmigration are critical steps in the establishment of distant metastasis by circulating tumor cells (CTCs). Also, vascular inflammation plays a pivotal role in steering CTCs out of the blood stream. Here, long circulating lipid-polymer nanoparticles encapsulating curcumin (NANOCurc) are proposed for modulating the vascular deposition of CTCs. Upon treatment with NANOCurc, the adhesion propensity of highly metastatic breast cancer cells (MDA-MB-231) onto TNF-α stimulated endothelial cells (HUVECs) reduces by ~ 70%, in a capillary flow. Remarkably, the CTC vascular deposition already reduces up to ~ 50% by treating solely the inflamed HUVECs. The CTC arrest is mediated by the interaction between ICAM-1 on HUVECs and MUC-1 on cancer cells, and moderate doses of curcumin down-regulate the expression of both molecules. This suggests that NANOCurc could prevent metastasis and limit the progression of the disease by modulating vascular inflammation and impairing the CTC arrest.

Keywords

Nanoparticles; Vascular inflammation; Metastasis; Cancer Prevention; Cell adhesion

Cancer cells can migrate from the primary malignant mass to distant sites through either the vascular compartment or the lymphatic system and generate secondary tumors, known as metastasis (1, 2). The metastatic cells are significantly different from their originators and tend to manifest resistance to any previously attempted therapeutic treatment (3-5).

*Correspondence: Department of Translational Imaging, Houston Methodist Research Institute, Houston, TX 77030, USA. Ph: +1 713 441 7316; Fax: +1 713 441 7316; pdecuzzi@houstonmethodist.org.

Conflict of Interests The authors declare no competing interests.

Appendix A. Supplementary Data Supplementary Materials and Methods and Supplementary Results can be found at ……

Consequently, about 90% of cancer deaths are caused by the progressive growth of metastatic nodules rather than the primary malignancy, and the detection of tumor cells in the peripheral circulation correlates well with low survival rates (6-8). The mechanisms regulating the dissemination of cancer cells are yet to be fully elucidated. However, cells moving through the vascular compartment – circulating tumor cells (CTCs) – are able to migrate away from the primary tumor, survive in the blood circulation, and eventually invade distant tissues via a process similar to the recruitment of leukocytes at loci of inflammation (9). Following this plausible mechanism, receptor molecules expressed over the CTC membrane would recognize counter-molecules on the endothelial cells and, eventually, the formation of stable intracellular molecular bonds would support the CTC capture from the blood stream (Figure.1A). Adhesion molecules associated with vascular inflammation, such as ICAM-1(10, 11), VCAM-1 (12), the selectin family (E- and P-selectin) (13, 14), have been often documented to support the vascular docking of CTCs. Notably, this correlates with several studies documenting that metastasis develop in a larger number and at higher rates in the presence of systemic and local inflammation (9, 15-21). Consequently, modulating inflammation at distant sites could play a major role in preventing metastasis and controlling the progression of the disease.

To this end, curcumin, a natural compound extracted from C*urcuma longa*, presents several interesting properties, including its potent anti-inflammatory activity (22, 23). Even if the NF-kB transcription factor has been shown to be the main target, curcumin can modulate the expression of a large number of proteins involved in tumor cell proliferation, adhesion, and migration (24, 25). Given the phenotypic heterogeneity of CTCs and cells in the metastatic nodules, the use of compounds with a broad-spectrum activity could offer distinct advantages over dedicated, single-target approaches (23). However, the administration of curcumin presents several unsolved challenges related to its hydrophobicity, poor adsorption, and bioavailability (26). As a consequence, huge doses of curcumin have been traditionally administered in preclinical and clinical studies for the treatment of cancer, providing often inconclusive and contradictory results. In pre-clinical studies on rats, an oral dose of 500 mg/kg resulted in a peak plasma concentration of only 1.8 ng/ml. In a phase II clinical trial, 25 patients with pancreatic cancer were administered daily with 8 g of curcumin leading to a maximum plasma level concentration of only 41 ng/ml. A significant inter-patient variability was also observed in terms of curcumin plasma concentration and therapeutic outcome (27, 28).

Nanoparticles (NPs) have been effectively used to enhance the bioavailability, improve the biodistribution and the therapeutic index of several compounds (29-31). Typically NPs comprise a core, where the active agent is loaded and protected by degradation, and a surface coating where ligand molecules can be attached to facilitate the recognition of specific cell populations. The NP geometry (size and shape) and physico-chemical properties can be finely tuned during their synthesis to optimize the loading and release of the compound (or multiple compounds), and to target specific organs and cell populations. For instance, spherical NPs with a diameter of a few hundreds of nanometers coated with stealth-polymers, such as polyethylene glycol (PEG), are typically associated with long circulation half-life and reduced sequestration by the immune system (32, 33). Preclinically,

NPs encapsulating curcumin have been used for the treatment of primary malignancies showing a decrease in tumor growth upon intratumor (34) (~1.0 mg/kg) and intraperitoneal (35) (~25 mg/kg) injection for pancreatic cancers; intravenous injection for colorectal cancer (~40 mg/kg) (36) and for melanoma (~2.0 mg/kg) (37).

In this study, the vascular deposition of tumor cells is modulated by using long-circulating lipid-polymer NPs for delivering moderate doses of curcumin to CTCs and inflamed endothelial cells. This “two-birds with one stone” approach, where the same NP formulation is attacking two different targets, would interrupt the metastatic cascade at its early stage, as schematically depicted in Figure.1B, and limit the spreading of the disease. More specifically, the rolling and adhesion behavior of highly metastatic triple negative breast cancer cells, MDA-MB-231, on TNF-α stimulated human umbilical vein endothelial cells (HUVECs) is studied using a parallel plate flow chamber system. Different treatment conditions are investigated with free curcumin and curcumin encapsulated into NPs (NANOCurc), on both MDA-MB-231 cells and HUVECs. Flow cytometry analysis and immunochemistry are used to dissect the biological mechanisms regulating the vascular adhesion and the cell response to curcumin treatments.

Materials and Methods

Materials and chemicals

Human Fibronectin was obtained from Sigma Aldrich (St. Louis, MO, USA). Curcumin (mixture of mixture of curcumin, demethoxycurcumin, and bisdemethoxycurcumin, 98+%) and Dimethyl sulfoxide (DMSO) were obtained from Fisher Scientific. XTT kit was obtained from Trevigen (Gaithersburg, Maryland 20877). Anti-human CD54 Purified, Anti-human CD227 (Mucin 1) eFluor615 (clone SM3), and Anti-mouse IgG1 APC, mouse IgG1 K Isotype control PE antibodies were obtained from e-biosciences; Anti-MUC1purified (clone SM3) was obtained from abcam. Recombinant human tumor Necrosis factor (TNF-α) was obtained from Sigma Aldrich. Phosphate buffered saline (PBS) and cell culture media were purchased from ATCC and PromoCell. PLGA (50:50, Carboxy Terminated, MW ~60 kDa) was purchased by Sigma Aldrich (St. Louis, MO). 1,2-dipalmitoyl-sn-glycero-3-phosphocholine (DPPC) and 1,2-distearoyl-sn-glycero-3-phosphoethanolamine-N-[succinyl(polyethylene glycol)-2000 (DSPE-PEG) and 1,2-dioleoyl-sn-glycero-3-phosphoethanolamine-N-(lissamine rhodamine B sulfonyl) were purchased by Avanti Polar Lipids (Alabaster, Alabama). Analytical grade dimethyl sulfoxide (DMSO), acetonitrile (ACN), chloroform and other solvents were obtained from Fisher Scientific.

Synthesis of nanoparticles encapsulating curcumin

1 mg of carboxy-terminated PLGA and 400 μg of Curcumin were dissolved in Chloroform to make an homogeneous solution. To create a lipid monolayer surrounding the particles two lipids were used: 1,2-dipalmitoyl-sn-glycero-3-phosphocholine (DPPC) and 1,2-distearoyl-sn-glycero-3-phosphoethanolamine-N-[succinyl(polyethylene glycol)-2000 (DSPE-PEG). The total amount of lipid used was the 20 % w/w of the amount of polymer used, in a DPPC/DSPE-PEG molar ratio of 7.5 to 2.5. To complete the oil phase, DPPC, because of its hydrophobicity, was added to the Curcumin-PLGA solution. The water phase was instead

made of DSPE-PEG dissolved in a 4 % ethanol solution, with a ratio between the oil phase and the water one of 1 to 5. Curcumin-loaded Nanoparticles were synthesized by using a single emulsion/solvent evaporation technique. Basically, the oil phase (PLGA+Curcumin in chloroform) was dropwise added to the water phase (DSPE-PEG in 4% ethanol), under ultrasonication. The formed emulsion was then gently stirred in a reduced pressure environment to facilitate the organic solvent evaporation. After the removal of all the organic solvent, Curcumin-loaded NPs were first centrifugated at a low speed to eliminate the synthesis debris (1000 × g for 2 minutes), then the supernatant was further purified by using Amicon Ultra filters (10 kDa molecular cut-off), to remove free drug and the eventual ethanol solution and to finally resuspend the particles in PBS. For the internalization studies, to the previous nanoparticles formulation, was also added a lipidconjugated rhodamine (1,2-dioleoyl-sn-glycero-3-phosphoethanolamine-N-(lissamine rhodamine B sulfonyl)), in the oil phase, by keeping the total lipid amount at 20 % w/w of the polymer and diminishing accordingly the DPPC amount.

Characterization of nanoparticles encapsulating curcumin

Curcumin-loaded nanoparticles were characterized by their size and morphology. The dynamic light scattering (DLS, Malvern Zetasizer Nano S) was used to measure the hydrondynamic size, while the scanning electron microscopy (SEM, FEI Nova NanoSEM 230) was used to assess the dried size. For the SEM measures, samples were prepared by drop casting and evaporation process in single side polished silicon wafer. The samples were then coated with platinum and analyzed at an accelerating voltage of 7 keV. For DLS measurements, to better understand nanoparticles stability, samples were kept at 37 °C, both in water and in PBS, and their size monitored for 7 days. For the drug loading and encapsulation efficiency, as for the release kinetics, the absorbance of Curcumin at 430 nm was used in order to calculate the molecule amount, taking as baseline the intensities of the same samples at 650 nm. Both for estimating the drug loading efficiency and the encapsulation efficiency, sample were first lyophilized, and then a known amount of nanoparticles were dissolved in acetonitrile for the spectrophotometer analyses or HPLC quantification (See Supplementary Materials). The drug loading efficiency was measured as the percentage amount in weight of Curcumin compared to the polymer mass. The encapsulation efficiency, on the other hand, was estimated as the percentage amount of Curcumin in an entire batch of the nanoparticle formulation compared to the initial amount of Curcumin used. For the release kinetics profile, 50 μl of nanoparticles solution were loaded into Slide-A-Lyzer MINI dialysis microtubes with a molecular cut off of 10 kDa (Pierce, Rockford, IL) and then dialyzed in 4 L of PBS buffer at pH 5 and pH 7.4 at 37 °C. The buffer was changed every 24 hours and at each time point considered, triplicate samples were individually collected and quantified.

Statistical analysis

Data are expressed as means ± SD. Before conducting the statistical analysis of significance, all data were analyzed for checking the presence of outliers using graphical-based boxplot outlier detection. Statistical significance of differences between means was determined by one-way ANOVA. Probability values of $p \leq 0.05$ were considered statistically significant

Results

Synthesis and physico-chemical characterization of nanoparticles encapsulating curcumin

Nanoparticles encapsulating curcumin molecules (NANOCurc) were synthesized using an emulsion/solvent evaporation technique, as detailed in the Materials and Methods. NANOCurc comprise a polymeric core, made of poly(lactic-co-glycolic acid) (PLGA); and an external layer, composed of a mixture of natural lipids and poly(ethylene glycol) (PEG) chains, as schematically depicted in the insets of Figure.1B. The curcumin molecules are dispersed within the hydrophobic PLGA core; whereas the outer layer serves to stabilize NANOCurc and enhance its circulation half-life. Note that these nanoparticles have been extensively characterized in vitro and in vivo, by the authors and other scientists, for different biomedical applications (38, 39). In particular, it has been shown that these lipid-polymer nanoparticles can have a circulation half-life of about 16h in small animal models (32).

After synthesis, the NANOCurc geometry was analyzed at the scanning electron microscope (SEM), as shown in Figure.2A, returning an average diameter of ~ 150 nm with a fairly monodisperse population. More relevant for biological application is the analysis of the NANOCurc size and its stability over time, performed with a dynamic light scattering system (DLS). The resulting data, presented in Figure.2B, show an average NANOCurc diameter of 171.6 ± 8.2 nm in DI water and 177.3 ± 6.2 nm in PBS, with a PDI of 0.174 ± 0.023 and 0.159 ± 0.026, respectively. Also the NANOCurc diameter is fairly constant under both conditions for 7 consecutive days at 37 °C. Only for the NANOCurc incubated in PBS, a small increase in average diameter of about 20% is registered after the first day. No additional variation in size is observed over the following 6 days of incubation. This variation in size should be related to the progressive surface adsorption of molecules dispersed in the buffer. Indeed, the small increase in size (~20%) cannot be ascribed to any NP clustering or lack of stability. NANOCurc stay well monodisperse for the whole duration of the incubation period (7 days), as confirmed by the PDI (Figure.2B). The loading and encapsulation efficiencies of curcumin into NANOCurc were quantified via spectrophotometric (Figure.2C) and HPLC analysis (Figure.S1). No significant difference was observed between the two methods, and the values for the two measured quantities are respectively ~ 6% and ~ 12%. Finally, the release profile of curcumin from NANOCurc is documented in Figure.2D showing the percentage of curcumin released over time under two different incubation conditions, namely in a physiological solution at pH = 7.4, mimicking the blood circulation; and in an acidic solution at pH = 5.0, mimicking the cell lysosomal environment. Within the first 5h, the profiles are similar and ~ 30% of the loaded curcumin is released. However, at longer time points, NANOCurc exposed to low pH tend to release from two to three times more curcumin than at pH = 7.4. Such a difference has to be ascribed to the PLGA degradation under acidic conditions, which is well documented in literature. Note also that the slower release at neutral pH is instrumental to the proper functioning of NANOCurc in that it limits the amount of curcumin loss in the circulation and maximizes the dose delivered to the target cells, upon endosomal localization.

Internalization of NANOCurc into Tumor and Endothelial Cells

Since curcumin is preferentially released upon nanoparticle internalization, it is crucial to analyze the cellular uptake of NANOCurc. A breast cancer cell line with high metastatic potential (MDA-MB-231 cells) is used as a model of circulating tumor cells; whereas human umbilical vein endothelial cells (HUVECs) are used as a model of cells lining the blood vessels. For the internalization study, the lipid layer covering the NANOCurc was labeled with a red fluorescent fluorophore, rhodamine. The internalization propensity of NANOCurc was assessed using two independent techniques: confocal microscopy and flow cytometry. Note that since curcumin fluoresces naturally in the green; NANOCurc (red spots) and curcumin (green spots) can be simultaneously detected.

For the confocal microscopy analysis, the MDA-MB-231 cells and HUVECs were exposed to 10 μM NANOCurc for ~1h. Figure.3 presents the results for the MDA-MB-231 cells, whereas data for the HUVECs are given in the Supplementary Materials (Figure.S2). In the left column of Figure.3, the first three different images show, respectively, the nucleus of the cells stained with DAPI (blue dye); the intracellular localization of the released curcumin (green dye) which appears to be quite uniformly distributed within the cytosol; and the NANOCurc (red dye) which show up as individualized dots mostly distributed perinuclearly. The last image presents an overlap of the three channels. The larger inset of Figure.3 gives a tridimensional reconstruction for the breast cancer cells showing that curcumin (green dye) and NANOCurc (red dye) are within the cell, and not just adhering on the cell membrane. It also shows well defined red dots corresponding to NANOcurc mostly localized in a perinuclear position and surrounded by a diffuse green fluorescent associated with the curcumin molecules slowly leaking out from NANOCurc and pervading the cell. In the Supplementary Materials, images of NANOCurc internalization and curcumin release are provided over multiple confocal planes (Figure.S10). In addition to the confocal microscopy analysis, flow cytometry was also performed to assess the intracellular accumulation of curcumin and NANOCurc at five different time points, namely 1, 2, 4, 6, 18, and 24h post incubation. The results are presented in the Supplementary Materials (Figure.S3) and confirm the cell uptake of NANOCurc and the progressive release of its cargo, curcumin. Notably, the flow cytometry data demonstrate that NANOCurc is more easily and rapidly internalized by endothelial cells stimulated with TNF-α (25 ng/ml) (Figure.S3B). These results support the notion that NANOCurc would preferentially accumulate into the inflamed endothelial cells as compared to the normal vasculature.

Cell cytotoxicity for free curcumin and NANOCurc

In order to avoid undesired off-site effects, the cytotoxic potential of curcumin on MDA-MB-231 cells and HUVECs is quantified using a XTT proliferative assay. The results are presented in Figure.4 and Figure.S4. It appears that the tumor cells, MDA-MB-231, are more resistant to curcumin than HUVECs. Consequently, the MDA-MB-231 cells were incubated with free curcumin or NANOCurc up to 40 μM and 72h; whereas the HUVECs were treated only up to 18h and 20 μM of curcumin, free or into NANOCurc. For both cell lines, the curcumin treatment affects the cell viability in a time and dose dependent manner (Figure.4). For the considered incubation period, cell proliferation is not affected at sufficiently low curcumin doses, namely up to ~ 20 μM for the MDAMB-231 cells and ~ 10

μM for the HUVECs. As the incubation time and dose increase, cell viability reduces giving for the MDA-MB-231 an IC_{50} of ~ 30 μM at 72h with free curcumin. For the HUVECs, an IC_{50} of ~ 10 μM was estimated by prolonging the incubation up to 72h (Figure.S4), thus confirming that endothelial cells are more susceptible to curcumin treatments. Overall, the treatment with NANOCurc presents lower cell toxicity than for the free curcumin treatment. This should be ascribed to the different availability and pharmacodynamics of curcumin: while free curcumin is immediately provided to the cells; NANOCurc must first be internalized by the cells, then its polymeric matrix progressively degrades slowly releasing curcumin over time which is eventually metabolized.

Effect of curcumin on the vascular adhesion of circulating tumor cells

A parallel plate flow chamber system (Figure.S5) is employed to analyze the CTC propensity to roll and adhere to the vascular endothelium under flow. This system is well established and has been extensively used to analyze the rolling and adhesion of leucocytes and circulating agents onto endothelial cells (40, 41). Treated and untreated MDA-MB-231 cells were injected in the flow chamber system as a model of circulating tumor cells; whereas a confluent layer of HUVECs was grown on the bottom of the chamber to mimic the blood vessel walls. HUVECs were treated with TNF-α to induce a local state of vascular inflammation. By processing the images acquired during the flow chamber experiments (Supplementary Movie.1), the number of firmly adhering circulating tumor cells n_{adh} was measured and normalized by the total number of injected cells n_{inj} and the area A of the region of interest. This ratio serves to quantify the propensity of the tumor cells to adhere to the vessel walls: the smaller is $n_{adh}/(n_{inj}\ A)$ and the lower is the CTC adhesion propensity. The bar chart in Figure.5A compares this ratio for three different treatment combinations with the control experiment (no treatment): MDA-MB-231 cells only treated with free curcumin (231+Curc); endothelial cells (HUVECs) only treated with free curcumin (EC +Curc); and both MDA-MB-231 and HUVECs treated with free curcumin (231+Curc/EC +Curc). Treating the breast cancer cells alone with 10 μM of curcumin for 24h and the HUVECs alone with 5 μM of curcumin for 1h lead to a ~ 50% reduction ($p < 0.01$) in vascular adhesion propensity of the MDA-MB-231. If both MDA-MB-231 cells and HUVECs are treated, at the same doses and times listed above, the vascular adhesion propensity reduces to ~ 70% ($p < 0.01$). Specifically, the values for the ratio $n_{adh}/(n_{inj}\ A)$ are 204.5 ± 70.24 #/m^2 for the control group (untreated cells); 118 ± 79 #/m^2 for the MDA-MB-231 cell treated only group; to 124.2 ± 66#/m^2 for the HUVEC treated only group; and 69.1 ± 21.3 #/m^2 in the case of tumor and endothelial cells being both treated with curcumin. In all cases, the HUVECs were first treated with curcumin and then stimulated for 6h with TNF-α at 25 ng/ml. Notably, no significant statistical difference is observed between the tumor cell only treated and the HUVEC only treated groups, and in both cases there is a remarkable 50% reduction in adhesion propensity.

Similar trends were observed with NANOCurc, as documented in Figure.5B. The vascular adhesion propensity of the MDA-MB-231 cells decreases as the concentration of NANOCurc increases. For MDA-MB-231 cells treated with 10 μM of NANOCurc for 24h and HUVECs exposed to 5 μM of NANOcurc for 2h, a reduction of 50% in vascular adhesion propensity is measured. As expected, this reduction is slightly lower than what

observed for free curcumin. A 70% reduction in vascular adhesion propensity ($p < 0.01$) is obtained by using 20 μM of NANOCurc on the MDA-MB-231 cells and HUVECs. More specifically, the ratio $n_{adh}/(n_{inj} \cdot A)$ was 111.8 ± 51.2 #/m^2 for 5 μM on HUVECs and 10 μM on MDA-MB-231 cells (10/5 μM); 91.3 ± 26 #/m^2 for 10 μM on HUVECs and MDA-MB-231 cells (10/10 μM); and dropped to 59.5 ± 24.5 #/m^2 for 20 μM on HUVECs and MDAMB-231 cells (20/20 μM in Figure.5).

In addition to the vascular adhesion propensity, the rolling velocity of the not adhering MDAMB-231 cells was also estimated as the distance traveled by the cell in a 10 second interval divided by time. The results are reported in Figure.5C. The simultaneous treatment of MDA-MB-231 cells (10 μM for 24h) and HUVECs (5 μM for 1h) with free curcumin induced a ~20% increase ($p < 0.01$) in rolling velocity. A similar variation was measured also for the MDA-MB-231 cells (20 μM for 24h) and HUVECs (20 μM for 2h) treated with NANOCurc ($p < 0.05$). Specifically, the rolling velocities for the untreated cells was 69.7 ±16.2 μm/s (Ctr) and it grows to 81.4 ± 17 μm/s for the cells treated with free curcumin (Curc), and 76.7 ±13.5 μm/s for the NANOCurc treatment (NANOCurc). Note that the adhesion propensity and rolling velocity are quantified using moderate doses of curcumin that would not induce any significant cell cytotoxicity.

Dissecting the mechanisms modulating the vascular adhesion of the circulating tumor cells

The intercellular adhesion molecule 1 (ICAM-1) is often involved in vascular adhesion processes and it is a well-established marker for vascular inflammation (10) . In order to elucidate the possible involvement of ICAM-1 on the firm adhesion of MDA-MB-231 cells, flow chamber experiments were performed using a TNF-α stimulated layer of HUVECs that were either treated with free curcumin (5 μM for 1h) or with an anti-ICAM-1 antibody (20 μg/ml for 30 min). The resulting adhesion propensity of the MDA-MB-231 cells is shown in Figure.5D. By blocking the ICAM-1 receptors on the HUVECs, the firm adhesion of the MDA-MB-231 cells is reduced by ~ 50%, which is comparable with the results obtained with free curcumin. This demonstrates that the expression of ICAM-1 on the inflamed endothelium can be modulated by a curcumin treatment and that ICAM-1 is indeed involved in the firm vascular adhesion of the MDA-MB-231 cells. Specifically, the treatment of the HUVECs with an anti-ICAM-1 antibody (20 μg/ml for 30 min) leads to an adhesion propensity ratio equal to 113.2 ± 32.3 #/m^2 which is quite similar to the value of 124.2 ± 66 #/m^2 obtained upon the free curcumin treatment of the HUVECs (5 μM for 1h).

Given the role played by ICAM-1, its expression on HUVECs was characterized using a flow cytometry analysis upon treatment with free curcumin and NANOCurc. Before each experiment, the HUVECs were stimulated with TNF-α at 25 ng/ml for 6 hours to increase the surface density of the ICAM-1 receptor. The flow cytometry data are shown in Figure. 6A and Figure.S7. These demonstrate that the curcumin treatment induces a time and dose dependent reduction in the expression of ICAM-1. Cells treated with 5 μM of free curcumin for 1h decrease the intensity of the fluorescent signal by about one order of magnitude, as compared to the positive controls (HUVECs not treated). A similar variation is also observed when incubating the HUVECs for 1h with 20 μM of NANOCurc.

Other authors have documented that the cell surface associated Mucin 1 molecule (MUC-1) could be involved in the adhesion process of tumor cells to the vascular walls (42-44). Therefore, an immunochemistry analysis was performed on the MDA-MB-231 cells to first confirm the presence of MUC-1 and then observe the effect of a curcumin treatment. For this analysis, an antibody targeting the under-glycosylated form of MUC-1(45) was chosen – the clone SM3 –, and after 7h of starvation, the breast cancer cells were treated for 24 hours with free curcumin and NANOCurc at 10 and 20 μM, respectively. Figure.6B shows the immunohistochemistry data: the negative control is the inset at the top left corner showing only the DAPI staining of the nucleii; in the top-right corner, the positive control is presented where the red fluorescence distributed throughout the cell is associated with the labeling of the MUC-1 cell glycoprotein. The two insets in the middle show the MDA-MB-231 cells after the treatment with free curcumin at 10 (left) and 20 μM (right), demonstrating a dose-dependent reduction in fluorescence, as compared with the positive control. Similar results are presented in the two insets at the bottom obtained for a treatment with 10 (left) and 20 μM (right) of NANOCurc. Moreover, flow cytometry analysis was performed on MDA-MB-231 to confirm the changes in expression of MUC-1 upon free curcumin and NANOCurc (10 μM/24h) treatment. FACS results show a decrease in underglycosylated MUC-1 in the treated cells, confirming the trends documented via immunohistochemistry (Figure.6B). Collectively, these results would suggest that the most plausible molecules dictating the firm adhesion of the MDA-MB-231 cells to the inflamed HUVECs are MUC-1 and ICAM-1; and the cellular expression of both molecules can be efficiently modulated by curcumin. However, this would not exclude the possible involvement of other inflammatory molecules, such as E-selectin, which have been shown to interact with MUC-1 and whose cell membrane expression is known to be down regulated by curcumin (24, 46).

Discussion

It is becoming clearer that systemic inflammation may influence the dissemination of tumor cells by facilitating the vascular arrest of CTCs and their proliferation at distant sites. In vivo studies document that the intravenous injection of LPS into mice may increase by over 40% the vascular deposition of lung carcinoma cells in hepatic sinusoids (16). Also, pulmonary inflammation was shown to enhance the formation of melanoma metastasis in the lungs by over 3 times (17). Furthermore, in obese individuals, the increased production of pro-inflammatory cytokines in the adipose tissue is known to induce a chronic inflammatory microenvironment that increases the metastatic potential (18, 19). Importantly, local and systemic inflammation are generated by the surgical removal of primary tumors, and this event is also inevitably associated with an increased number of circulating tumor cells (20). Very recently, it has been observed that CTCs can be sequestered from the blood stream by neutrophil extracellular traps, which originate in response to inflammatory cues, thus facilitating the colonization of distant organs (21). It is also documented that both CTCs and immune cells, recruited or residing at the tumor site, tend to release in the circulation pro-inflammatory cytokines inducing the over-expression of endothelial molecules such as ICAM-1, VCAM-1 and E/P-selectins (9, 15). In several studies, such inflammatory molecules have been documented to be involved in the vascular deposition and arrest of

different types of tumor cells (12, 47). These observations would suggest a fundamental correlation between vascular inflammation and the initiation and progression of the metastatic disease.

Considering that CTCs and metastasis are phenotypically different from the primary tumor cells (4, 5) and in view of the major role played by local and systemic inflammation, an effective strategy for limiting the distant spreading of tumor cells could be that of interrupting the process at its early stage by modulating the propensity of CTCs to adhere to the vasculature (Figure.1). In this work, this has been demonstrated by using a “two-birds with one stone” approach where a NP encapsulating curcumin (NANOCurc - Figure.2) hits two different targets: the circulating tumor cells and the inflamed endothelium. The internalization of NANOCurc in the tumor (MDA-MB-231) and endothelial (HUVECs) cells would trigger the release of curcumin, via the progressive hydrolysis of the polymeric PLGA matrix in the lysosomal environment (Figure.3). On the other hand, the surface coating of NANOCurc, comprising a single lipid layer and PEG chains, would provide a long circulation half-life, as already documented (32). This is a crucial property for NANOCurc in that it would enhance the probability of encountering CTCs in the blood stream, which is indeed a rare event (1 CTC per 10^6-10^9 blood cells). Moderate doses of curcumin, that would not induce any appreciable cytotoxicity (Figure.4), provided to the tumor cells and the inflamed endothelium would reduce the propensity for vascular adhesion of the MDA-MB-231 by ~ 70% (Figure.5). Furthermore, NANOCurc was shown to be preferentially uptaken by the inflamed endothelium (Supplementary Materials and Figure.S3), and to induce already a remarkable ~ 50% reduction in vascular adhesion of CTCs. It should be emphasized that NANOCurc, as most nanoparticles, would also be uptaken by phagocytic cells, including circulating monocytes and organ specific macrophages. The slow release of curcumin from NANOCurc within phagocytic cells would modulate the inflammatory state of these cells and potentially induce a systemic beneficial effect. In particular, curcumin will decrease the expression of three cytokines, namely IL-1β, IL-6, and IL-10 (Figure.S9), that are often associated with cancer inflammation and progression (15, 48, 49).

Finally, it should be emphasized that the proposed nanoparticle can be readily modified to include targeting moieties for enhancing specificity, additional therapeutic agents for multi-drug therapies (50), and contrast agents for intratissue localization in real time (38).

In conclusion, this study demonstrates that the firm arrest of circulating breast cancer cells (MDA-MB-231) onto the inflamed endothelium can be efficiently modulated by using long-circulating nanoparticles (NANOCurc) encapsulating a natural anti-inflammatory compound, such as curcumin. Vascular adhesion is primarily mediated by the specific interaction between ICAM-1 on the endothelial cells and MUC-1 on the breast cancer cells. Treatments of the inflamed endothelium and CTCs with moderate doses of NANOCurc decrease by 70% the number of adhering tumor cells. Furthermore, a 50% decrease in vascular adhesion can already be achieved by just targeting NANOCurc to the inflamed endothelium. NANOCurc could represent a new therapeutic strategy to prevent the formation of metastasis, for instance upon surgical removal of a primary tumor, and limit the progression of the disease by attacking simultaneously the CTCs and vascular inflammation.

Supplementary Material

Refer to Web version on PubMed Central for supplementary material.

Acknowledgments

Grants This work was partially supported by the Cancer Prevention Research Institute of Texas through the grant CPRIT RP110262; the National Institutes of Health (NIH, USA) through the grants U54CA143837 and U54CA151668. Anna L. Palange and Daniele Di Mascolo acknowledge the Doctoral School of The University of Magna Graecia (Italy) for travel support. Daniele Di Mascolo also acknowledges the support of the EU Commission, the European Social Fund and the department 11 “Culture - Education - University - Research - Technological Innovation – Higher Education” of Calabria Region (POR Calabria FSE 2007/2013).

References

1. Chaffer CL, Weinberg RA. A perspective on cancer cell metastasis. Science. 2011; 331:1559–64. [PubMed: 21436443]
2. Kang Y, Pantel K. Tumor Cell Dissemination: Emerging Biological Insights from Animal Models and Cancer Patients. Cancer cell. 2013; 23:573–81. [PubMed: 23680145]
3. Fidler IJ. The pathogenesis of cancer metastasis: the ‘seed and soil’ hypothesis revisited. Nature Reviews Cancer. 2003; 3:453–8.
4. Mego M, Mani SA, Cristofanilli M. Molecular mechanisms of metastasis in breast cancer—clinical applications. Nature reviews Clinical oncology. 2010; 7:693–701.
5. Yu M, Bardia A, Wittner BS, Stott SL, Smas ME, Ting DT, et al. Circulating breast tumor cells exhibit dynamic changes in epithelial and mesenchymal composition. science. 2013; 339:580–4. [PubMed: 23372014]
6. Cristofanilli M, Budd GT, Ellis MJ, Stopeck A, Matera J, Miller MC, et al. Circulating tumor cells, disease progression, and survival in metastatic breast cancer. New England Journal of Medicine. 2004; 351:781–91. [PubMed: 15317891]
7. Ghazani AA, McDermott S, Pectasides M, Sebas M, Mino-Kenudson M, Lee H, et al. Comparison of select cancer biomarkers in human circulating and bulk tumor cells using magnetic nanoparticles and miniaturized micro-NMR system. Nanomedicine: Nanotechnology, Biology and Medicine. 2013 (In press).
8. Grobmyer SR, Zhou G, Gutwein LG, Iwakuma N, Sharma P, Hochwald SN. Nanoparticle delivery for metastatic breast cancer. Maturitas. 2012; 73:19–26. [PubMed: 22402026]
9. Miles FL, Pruitt FL, van Golen KL, Cooper CR. Stepping out of the flow: capillary extravasation in cancer metastasis. Clinical & experimental metastasis. 2008; 25:305–24. [PubMed: 17906932]
10. Yang L, Froio RM, Sciuto TE, Dvorak AM, Alon R, Luscinskas FW. ICAM-1 regulates neutrophil adhesion and transcellular migration of TNF-α-activated vascular endothelium under flow. Blood. 2005; 106:584–92. [PubMed: 15811956]
11. Kawai Y, Kaidoh M, Ohhashi T. MDA-MB-231 produces ATP-mediated ICAM-1-dependent facilitation of the attachment of carcinoma cells to human lymphatic endothelial cells. American Journal of Physiology-Cell Physiology. 2008; 295:C1123–C32. [PubMed: 18768924]
12. Liang S, Dong C. Integrin VLA-4 enhances sialyl-Lewisx/a-negative melanoma adhesion to and extravasation through the endothelium under low flow conditions. American Journal of Physiology-Cell Physiology. 2008; 295:C701–C7. [PubMed: 18632734]
13. Läubli, H.; Borsig, L. Seminars in cancer biology. Vol. 20. Elsevier; 2010. Selectins promote tumor metastasis; p. 169-77.
14. Tremblay P-L, Huot J, Auger FA. Mechanisms by which E-selectin regulates diapedesis of colon cancer cells under flow conditions. Cancer research. 2008; 68:5167–76. [PubMed: 18593916]
15. Borsig L, Wolf M, Roblek M, Lorentzen A, Heikenwalder M. Inflammatory chemokines and metastasis—tracing the accessory. Oncogene. 2013 (In press).

16. McDonald B, Spicer J, Giannais B, Fallavollita L, Brodt P, Ferri LE. Systemic inflammation increases cancer cell adhesion to hepatic sinusoids by neutrophil mediated mechanisms. International Journal of Cancer. 2009; 125:1298–305.

17. Taranova AG, Maldonado D, Vachon CM, Jacobsen EA, Abdala-Valencia H, McGarry MP, et al. Allergic pulmonary inflammation promotes the recruitment of circulating tumor cells to the lung. Cancer research. 2008; 68:8582–9. [PubMed: 18922934]

18. Calle EE, Rodriguez C, Walker-Thurmond K, Thun MJ. Overweight, obesity, and mortality from cancer in a prospectively studied cohort of US adults. New England Journal of Medicine. 2003; 348:1625–38. [PubMed: 12711737]

19. Iyengar, NM.; Morris, PG.; Hudis, CA.; Dannenberg, AJ. Obesity, Inflammation and Cancer. Springer; 2013. Obesity, Inflammation, and Breast Cancer; p. 181-217.

20. Sawabata N, Okumura M, Utsumi T, Inoue M, Shiono H, Minami M, et al. Circulating tumor cells in peripheral blood caused by surgical manipulation of non-small-cell lung cancer: pilot study using an immunocytology method. General thoracic and cardiovascular surgery. 2007; 55:189–92. [PubMed: 17554991]

21. Cools-Lartigue J, Spicer J, McDonald B, Gowing S, Chow S, Giannias B, et al. Neutrophil extracellular traps sequester circulating tumor cells and promote metastasis. The Journal of clinical investigation. 2013; 123:3446.

22. Shehzad A, Rehman G, Lee YS. Curcumin in inflammatory diseases. BioFactors. 2012

23. Kunnumakkara AB, Anand P, Aggarwal BB. Curcumin inhibits proliferation, invasion, angiogenesis and metastasis of different cancers through interaction with multiple cell signaling proteins. Cancer letters. 2008; 269:199–225. [PubMed: 18479807]

24. Zhou H, Beevers CS, Huang S. Targets of curcumin. Current drug targets. 2011; 12:332. [PubMed: 20955148]

25. Chen H-W, Lee J-Y, Huang J-Y, Wang C-C, Chen W-J, Su S-F, et al. Curcumin inhibits lung cancer cell invasion and metastasis through the tumor suppressor HLJ1. Cancer research. 2008; 68:7428–38. [PubMed: 18794131]

26. Sharma RA, McLelland HR, Hill KA, Ireson CR, Euden SA, Manson MM, et al. Pharmacodynamic and pharmacokinetic study of oral Curcuma extract in patients with colorectal cancer. Clinical Cancer Research. 2001; 7:1894–900. [PubMed: 11448902]

27. Dhillon N, Aggarwal BB, Newman RA, Wolff RA, Kunnumakkara AB, Abbruzzese JL, et al. Phase II trial of curcumin in patients with advanced pancreatic cancer. Clinical Cancer Research. 2008; 14:4491–9. [PubMed: 18628464]

28. Ireson C, Orr S, Jones DJ, Verschoyle R, Lim C-K, Luo J-L, et al. Characterization of metabolites of the chemopreventive agent curcumin in human and rat hepatocytes and in the rat in vivo, and evaluation of their ability to inhibit phorbol ester-induced prostaglandin E2 production. Cancer Research. 2001; 61:1058–64. [PubMed: 11221833]

29. Peer D, Karp JM, Hong S, Farokhzad OC, Margalit R, Langer R. Nanocarriers as an emerging platform for cancer therapy. Nature nanotechnology. 2007; 2:751–60.

30. Ryu JH, Koo H, Sun I-C, Yuk SH, Choi K, Kim K, et al. Tumor-targeting multi-functional nanoparticles for theragnosis: new paradigm for cancer therapy. Advanced drug delivery reviews. 2012; 64:1447–58. [PubMed: 22772034]

31. Koo OM, Rubinstein I, Onyuksel H. Role of nanotechnology in targeted drug delivery and imaging: a concise review. Nanomedicine: Nanotechnology, Biology and Medicine. 2005; 1:193–212.

32. Hu C-MJ, Zhang L, Aryal S, Cheung C, Fang RH, Zhang L. Erythrocyte membrane-camouflaged polymeric nanoparticles as a biomimetic delivery platform. Proceedings of the National Academy of Sciences. 2011; 108:10980–5.

33. Moghimi SM, Hunter AC, Murray JC. Nanomedicine: current status and future prospects. The FASEB Journal. 2005; 19:311–30.

34. Yallapu MM, Ebeling MC, Khan S, Sundram V, Chauhan N, Gupta BK, et al. Novel Curcumin Loaded Magnetic Nanoparticles for Pancreatic Cancer Treatment. Molecular cancer therapeutics. 2013; 12:1471–80. [PubMed: 23704793]

35. Bisht S, Mizuma M, Feldmann G, Ottenhof NA, Hong S-M, Pramanik D, et al. Systemic administration of polymeric nanoparticle-encapsulated curcumin (NanoCurc) blocks tumor growth and metastases in preclinical models of pancreatic cancer. Molecular cancer therapeutics. 2010; 9:2255–64. [PubMed: 20647339]
36. Li L, Ahmed B, Mehta K, Kurzrock R. Liposomal curcumin with and without oxaliplatin: effects on cell growth, apoptosis, and angiogenesis in colorectal cancer. Molecular cancer therapeutics. 2007; 6:1276–82. [PubMed: 17431105]
37. Lin Y-L, Liu Y-K, Tsai N-M, Hsieh J-H, Chen C-H, Lin C-M, et al. A Lipo-PEG-PEI complex for encapsulating curcumin that enhances its antitumor effects on curcumin-sensitive and curcumin-resistance cells. Nanomedicine: Nanotechnology, Biology and Medicine. 2012; 8:318–27.
38. Aryal S, Key J, Stigliano C, Ananta JS, Zhong M, Decuzzi P. Engineered magnetic hybrid nanoparticles with enhanced relaxivity for tumor imaging. Biomaterials. 2013; 34:7725–32. [PubMed: 23871540]
39. Zhang L, Chan JM, Gu FX, Rhee J-W, Wang AZ, Radovic-Moreno AF, et al. Self-assembled lipid–polymer hybrid nanoparticles: a robust drug delivery platform. Acs Nano. 2008; 2:1696–702. [PubMed: 19206374]
40. Lawrence MB, Springer TA. Leukocytes roll on a selectin at physiologic flow rates: distinction from and prerequisite for adhesion through integrins. Cell. 1991; 65:859–73. [PubMed: 1710173]
41. Adriani G, de Tullio MD, Ferrari M, Hussain F, Pascazio G, Liu X, et al. The preferential targeting of the diseased microvasculature by disk-like particles. Biomaterials. 2012; 33:5504–13. [PubMed: 22579236]
42. Regimbald LH, Pilarski LM, Longenecker BM, Reddish MA, Zimmermann G, Hugh JC. The breast mucin MUC1 as a novel adhesion ligand for endothelial intercellular adhesion molecule 1 in breast cancer. Cancer research. 1996; 56:4244–9. [PubMed: 8797599]
43. Ciborowski P, Finn OJ. Non-glycosylated tandem repeats of MUC1 facilitate attachment of breast tumor cells to normal human lung tissue and immobilized extracellular matrix proteins (ECM) in vitro: potential role in metastasis. Clinical & experimental metastasis. 2002; 19:339–45. [PubMed: 12090474]
44. Shen Q, Rahn JJ, Zhang J, Gunasekera N, Sun X, Shaw AR, et al. MUC1 Initiates Src-CrkLRac1/Cdc42–Mediated Actin Cytoskeletal Protrusive Motility after Ligating Intercellular Adhesion Molecule-1. Molecular Cancer Research. 2008; 6:555–67. [PubMed: 18403635]
45. Kufe DW. Mucins in cancer: function, prognosis and therapy. Nature Reviews Cancer. 2009; 9:874–85.
46. Geng Y, Yeh K, Takatani T, King MR. Three to tango: MUC1 as a ligand for both E-selectin and ICAM-1 in the breast cancer metastatic cascade. Frontiers in oncology. 2012; 2
47. Dianzani C, Brucato L, Gallicchio M, Rosa A, Collino M, Fantozzi R. Celecoxib modulates adhesion of HT29 colon cancer cells to vascular endothelial cells by inhibiting ICAM-1 and VCAM-1 expression. British journal of pharmacology. 2008; 153:1153–61. [PubMed: 18084316]
48. Pollard JW. Tumour-educated macrophages promote tumour progression and metastasis. Nature Reviews Cancer. 2004; 4:71–8.
49. Qian B-Z, Pollard JW. Macrophage diversity enhances tumor progression and metastasis. Cell. 2010; 141:39–51. [PubMed: 20371344]
50. Aryal S, Hu C-MJ, Zhang L. Polymeric nanoparticles with precise ratiometric control over drug loading for combination therapy. Molecular pharmaceutics. 2011; 8:1401–7. [PubMed: 21696189]

Tumor cells adhere to the vessel walls and migrate across the endothelium to colonize distant sites. Vascular adhesion molecules, such as ICAM-1 and E-selectin, support the interaction of circulating tumor cells with the inflamed endothelium facilitating cell extravasation. Long circulating nanoparticles loaded with curcumin, a potent anti-inflammatory natural product, can modulate the expression of adhesion molecules on both the circulating tumor cells and the inflamed endothelium thus reducing the likelihood of metastasis formation.

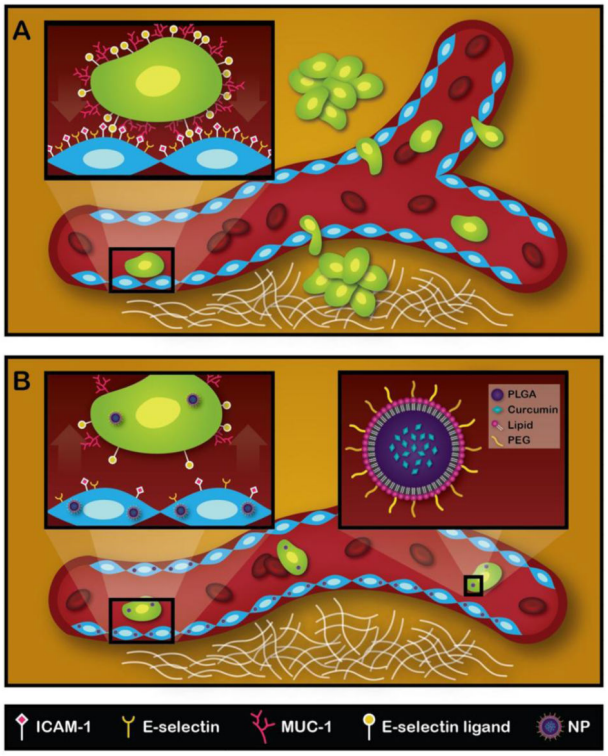

Figure.1. Schematic representation of the metastatic process and mechanism of action for NANOCurc

A. CTCs adhering to the vessel walls and migrating across the endothelium to form secondary tumor masses. In the inset, a tumor cell is specifically interacting with endothelial cells via membrane adhesion molecules. **B**. Following NANOCurc treatment, the expression of adhesion molecules on the CTCs (MUC-1) and inflamed endothelium (ICAM-1) is reduced thus limiting the number of metastasis. In the inset, NANOCurc is schematically presented including its PLGA core, encapsulating curcumin, and its surface coating, obtained by combining lipids and PEG chains.

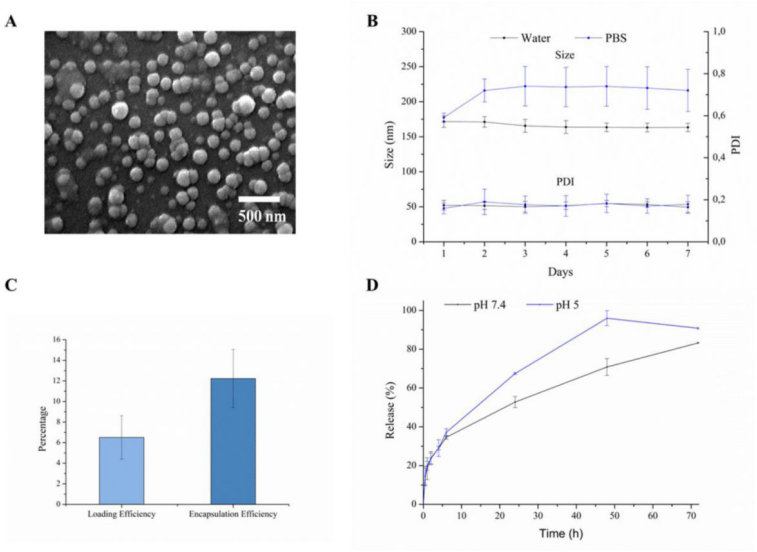

Figure.2. Physico-chemical characterization of NANOCurc

A. SEM image of NANOCurc showing a monodisperse population with an average ~150 nm diameter. **B.** DLS measurements of NANOCurc diameter (up) and polydispersity index (PDI – bottom) over time in two different solutions (DI water and PBS). **C**. Loading (Curc weight/NANOCurc weight) and encapsulation efficiencies (NANOCurc drug cargo/input drug) for NANOCurc. **D**. Curcumin release profiles under physiological (pH 7.4, black squares) and acidic (pH 5.0, blue dots) conditions.

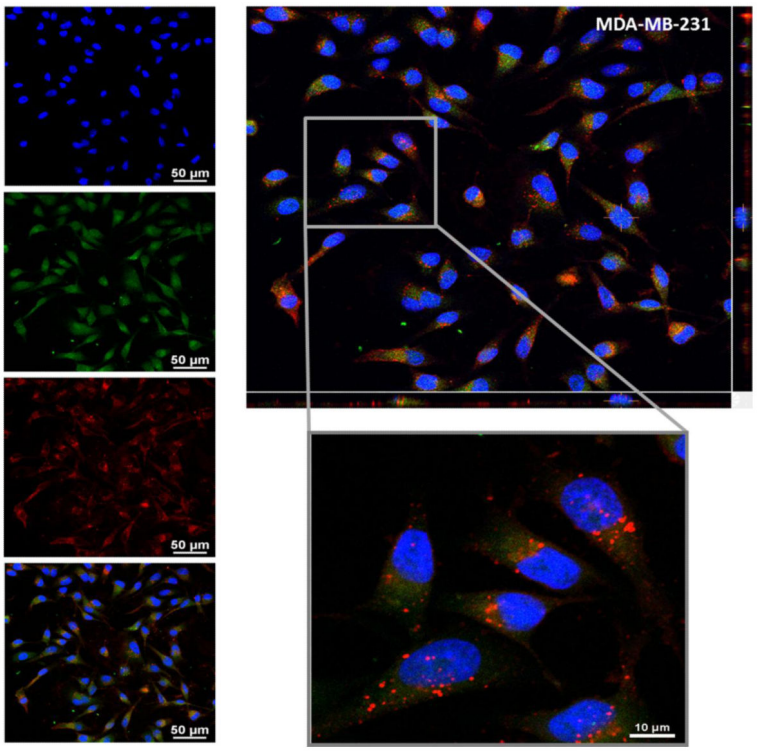

Figure.3. NANOCurc internalization in MDA-MB-231 cells

Confocal microscopy images of the MDA-MB-231 cells after 1 hour incubation with 10 µM of Rhodamine-labeled NANOCurc. On the left, from top to bottom, images showing a DAPI nuclear staining (blue), curcumin distribution (green), and NANOCurc distribution (red) in the MDA-MB-231 cells; and the merged picture. On the top right, confocal Z-stack analysis demonstrating that NANOCurc is internalized by the cancer cells.

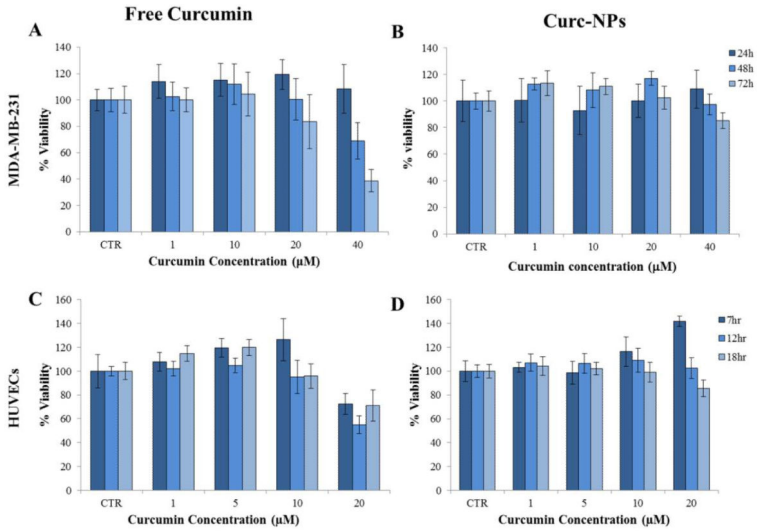

Figure.4. Cytotoxicity analysis with free curcumin and NANOCurc

(A-B) Viability for the MDA-MB-231 cells and **(C-D)** HUVECs exposed at different doses and different incubation times to free curcumin and NANOCurc (n= 25).

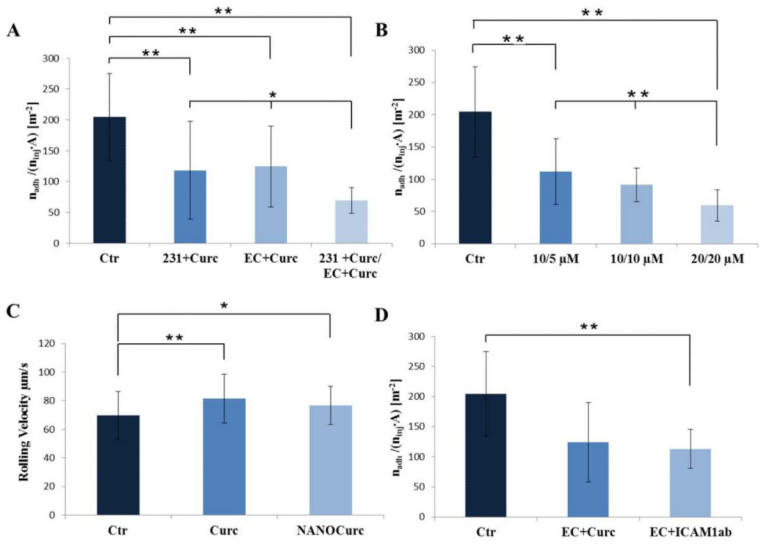

Figure.5. Vascular adhesion and rolling velocity of cancer cells on the inflamed endothelium

A. Adhesion propensity of the MDA-MB-231 cells in the case of no curcumin treatment (Ctr); MDA-MB-231 cells only treated with free Curc (10 μM for 24h) **(**231+Curc**)**; HUVECs only treated with free Curc (5 μM for 1h) **(**EC+Cur**);** MDA-MB-231 cells and HUVECs treated with free Curc (10 μM for 24h; 5 μM for 1h, respectively) **(**231+Curc/EC +Curc**). B.** Adhesion propensity of the MDA-MB-231 cells in the case of no curcumin treatment (Ctr); MDA-MB-231 cells and HUVECs treated with NANOCurc (10 μM for 24h; 5 μM for 2h, respectively) **(**10/5μM**)**; MDA-MB-231 cells and HUVECs treated with NANOCurc (10 μM for 24h; 10 μM for 2h, respectively) (10/10μM); MDA-MB-231 cells and HUVECs treated with NANOCurc (20 μM for 24h; 20 μM for 2h, respectively) (20/20μM). **C.** Rolling velocity of the MDA-MB-231 cells in the case of no curcumin treatment (Ctr)**;** MDA-MB-231 cells and HUVECs treated with free curcumin (10 μM for 24h, 5 μM for 1h, respectively) (Curc); MDA-MB-231 cells and HUVECs treated with NANOCurc (20 μM for 24h, 20 μM for 2h, respectively) (NANOCurc). **D.** Adhesion propensity of the MDA-MB-231 cells in the case of no curcumin treatment (Ctr); HUVECs only treated with free curcumin (5 μM for 1h) (EC+Curc); HUVECs incubated with Anti-ICAM-1 antibody (ICAM-1Ab).

In all experiments, HUVECs were stimulated with TNF-α at 25 ng/ml for 6h. The adhesion propensity is quantified as the ratio between the number of firmly adhering cells (n_{adh}), the total number of injected cells ($n_{inj} = 10^6$) and the area of the region of interest ($A = 0.33\times10^{-6}$ m^2). Data are plotted as mean ± SD. The symbol " * " denotes statistically significant difference at $p \leq 0.05$, as compared to control (Ctr). The symbol " ** " denotes statistically significant difference at $p \leq 0.01$, as compared to control (Ctr). (n ≥ 10 for each tested condition).

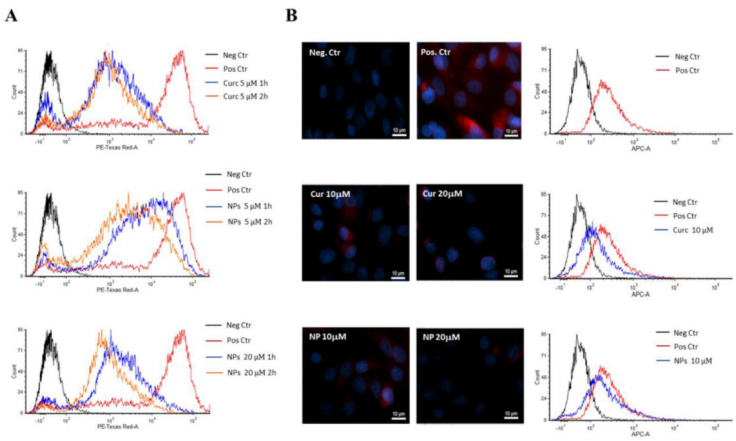

Figure.6. Flow cytometry and immunochemistry analysis for the adhesion molecules A

Flow cytometry analysis for the ICAM-1 expression on HUVECs stimulated with TNF-α (Positive Control – red line); treated with free curcumin at 5 μM for 1h (blue line) and at 5 μM for 2 h (orange line) (up); treated with NANOCurc at 5 μM for 1h (blue line) and at 5 μM for 2h (orange line) (middle); and treated with NANOCurc at 20 μM for 1 (blue line) and at 20 μM 2h (orange line) (bottom). Fluorescence signals of positive control and treated cells were compared to negative control (black line) **B.** Immunochemistry analysis for the expression of MUC-1 on MDA-MB-231 cells: negative control (top left), positive control (top right); curcumin treated cells at 10 μM (middle, left) and 20 μM (middle, right); NANOCurc treated cells at 10 μM (bottom, left) and 20 μM (bottom, right). **C.** Flow cytometry analusis of the expression of MUC-1 on MDA-MB-231 in the case of no curcumin treatment (Pos. Ctr – red line); treated with free curcumin at 10 μM (blue line, middle graph), and treated with NANOCurc at 10 μM (blue line, bottom graph). Fluorescence signals of Pos. Ctr and treated cells were compared to Neg. Ctr (black line).